

The albatross optimized flight is an extremum seeking phenomenon: autonomous and stable controller for dynamic soaring

Sameer Pokhrel and Sameh A. Eisa

Abstract. The albatross optimized flight maneuver – known as Dynamic Soaring (DS) – is nothing but a wonder of physics, biology, and engineering. In an ideal DS cycle, this fascinating bird can travel in the desired flight direction, for free, by harvesting energy from the wind, and hence, it achieves a neutral energy cycle. This phenomenon has triggered a momentous interest among aeronautical, control and robotic engineering communities; if DS is mimicked, we have arrived at a new class of Unmanned Aerial Vehicles (UAVs) which are very energy-efficient during part (or the full) duration of their flight. However, the DS problem is highly nonlinear, under-actuated, and dependent on the wind profiles. This has resulted in decades of DS control literature that, while making progress in addressing the control problem, seem not to be aligned well with the nature of the DS phenomenon itself. The control works associated with DS in the literature rely heavily on constrained optimal control algorithms, control designs that require a mathematical expression of the objective function, and predefined wind profile models. Clearly, a functioning controller for DS that allows meaningful bio-mimicry of the albatross, needs to be autonomous, real-time, stable, and capable of tolerating the absence of the expression of the objective function (similar to what the bird does). The qualifications of such controller are the very same characteristics of Extremum Seeking Control (ESC) systems. In this paper, we show that ESC systems existing in control literature for decades are a natural characterization of the DS problem. We provide the DS problem setup, design, stability, and simulation results of the introduced ESC systems. The results, supported by comparison with optimal control solvers, emphasize that the DS phenomenon is a natural expression of ESC systems in nature and that DS can be performed autonomously and in real-time with stability guarantees.

LIST OF SYMBOLS AND ABBREVIATIONS

<i>DS</i>	Dynamic Soaring
<i>ESC</i>	Extremum Seeking Control
<i>UAVs</i>	Unmanned Aerial Vehicles
<i>x</i>	Position vector along East direction
<i>y</i>	Position vector along North direction
<i>z</i>	Altitude
<i>V</i>	Airspeed
γ	Air relative flight path angle
ψ	Air relative heading angle

ϕ	Bank angle
C_L	Coefficient of Lift
C_D	Coefficient of Drag
L	Aerodynamic Lift
D	Aerodynamic Drag
ρ	Air density
S	Wing area
m	Mass of UAV/albatross
n	Load factor
$SISO$	Single input single output
K	Induced drag coefficient
W_0	Free stream wind speed
δ	Shear layer thickness
PE	Potential energy
KE	Kinetic energy
TE	Total energy
DC	Direct collocation
W	Wind velocity
\dot{W}	Wind shear gradient
T_{cyc}	Time period for a single cycle
g	Acceleration due to gravity

1. Introduction

Dynamic Soaring (DS) maneuver is a fascinating flight strategy that utilizes wind gradients to perform long-duration flights by harvesting atmospheric energy [1, 2]. The energy needed to perform such a long duration of the flight is gained from the wind in the proximity of the surface. In regions above the sea surface or mountainous areas, the speed of the horizontal wind changes considerably with the altitude to yield what is known as “wind shear” [3, 4]. By flying across the wind gradient region periodically, energy is harvested from the spatial wind speed distribution. This has been observed amongst what is known as soaring birds (albatrosses, eagles, etc.). As a matter of fact, the DS maneuver enables soaring birds to travel large distances almost without flapping their wings as energy spending is minimized substantially [5]. The DS cycle can be considered to have four characteristic flight phases [4], namely (a) windward climb, (b) high altitude turn, (c) tailwind descent, and (d) low altitude turn – see figure 1. In order to conduct this maneuver, the bird goes into the headwind and gains height – trading off kinetic energy with potential energy – and at the highest point, it takes a steep turn and dives down with tailwind. It continues to descend – trading off potential energy with kinetic energy – and obtain gains in the velocity until it reaches the minimum possible height. At that point, it takes the low altitude turn and starts a new DS cycle. Ideally, the DS cycle is an energy-neutral maneuver. As a matter of fact, the DS phenomenon

has been verified and validated experimentally [3, 6].

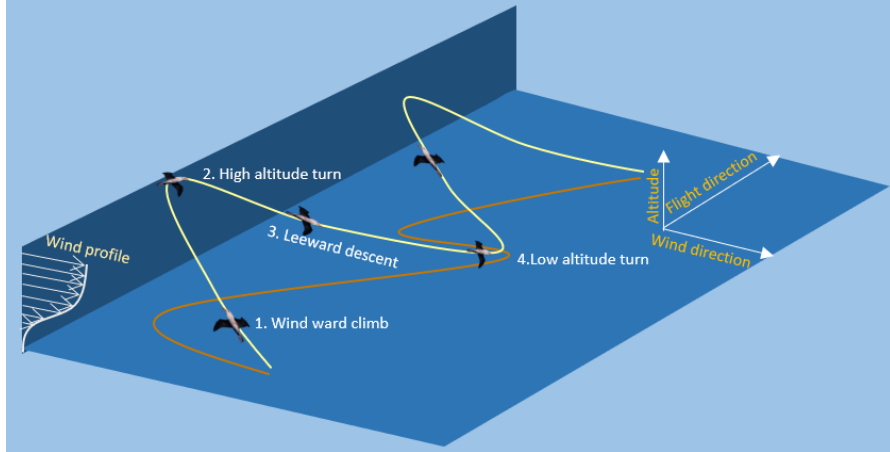


Figure 1. Dynamic soaring maneuver with logistic wind profile.

The interest in albatross flight secret goes back to Leonardo da Vinci [7] hundreds of years ago. This interest is still present today, particularly in the aeronautical, robotic and control engineering communities. If one will be able to mimic soaring birds, then substantial advancements can be projected on Unmanned Aerial Vehicles (UAVs) and bio-inspired robotics. In order to do such a complex bio-mimicry, researchers tried to study the control structures, designs, methods, and techniques that will allow the application of DS in real life, especially in UAVs flight [8, 9, 10, 11]. However, as documented in the review work [4], most of the control literature on DS is characterized as an optimal control problem, in part or in full. That is, the objective of the DS problem is to identify or find an optimal control trajectory through which the flight is energy neutral, or near-neutral [12, 13, 1, 14]. It is important to emphasize that such optimal control and trajectory planning problems are not real-time and very dependent on the models of the wind shear assumed during the conduction of the optimization methods/algorithms/solvers. Recently, a dynamic soaring simulation system has been developed that contains an online estimation and control stage utilizing an offline training framework [15]. Nevertheless, said methods, optimal control-based frameworks, or suggested control-designs/trajectory-planning, are not real-time and require the mathematical expression of the objective function and wind shear models to be known *a priori*. Moreover, the DS problem setup in all mentioned contributions in literature usually necessitate heavy constraints and bound, which have to be imposed [4]. Very recently, it is shown that optimal control inputs – determined by optimal control methods – applied to the DS system dynamics provide an unstable system [16, 17].

Motivation to find an alternative controller methodology that captures the nature of the problem: It is quite clear that the control methods of the DS problem in literature lead to systems that are one or more of the following: (1) non-real-time, (2) computationally complex and expensive, (3) unstable, and (4) very model-dependent (the objective function and wind profile models have to be known *a priori*).

By looking at the literature on autonomous control systems, one adaptive controller system stands out. This controller system is very descriptive and natural to the DS problem: the Extremum Seeking Control (ESC) systems [18]. These extremum seeking systems operate by steering a dynamical system – such as the albatross or a mimicking UAV – to the extremum (maximum or minimum) of an objective function or optimal state – such as maximum energy gain or minimum energy spending – without requiring access to the mathematical expression of the objective function; ESC systems are operable by having access to measurements of the objective function, and not necessarily its mathematical expression. Additionally, ESC systems have been proven stable, real-time, and autonomous [19, 20, 21]. What is also interesting about ESC systems is that they tolerate less than properly modeled dynamics as long as the objective function can be measured accurately; this is fitting to bio-mimicking modeling in general and the DS problem in particular. The reader is directed to the first chapter in the reference [22] for detailed account of classic ESC structures. ESC systems have been proven applicable in many engineering disciplines such as formation flight [23], autonomous vehicles [24, 25], solar array optimization [26, 27], anti-lock braking system [28, 29], mobile robots [30], bio-mimicry of fish source seeking [31, 32], among many others.

Contribution: In this paper we provide: (1) a novel characterization of the albatross optimized flight maneuver – the DS phenomenon – as an autonomous real-time extremum seeking system, (2) implementation of two ESC structures incorporating the DS problem, (3) stability analysis of the ESC system characterizing successful energy-neutral DS cycle, and (4) a comparison between the results of the ESC systems used in the implementation with the solutions of two numerical optimizers: GPOPS2 [33] and Direct Collocation-based method (DC) [14]. In addition to the contributions directly related to the DS problem, it is important to note that, this work, to the best of our knowledge, is the first to bring ESC systems to the field of bird flights and bio-inspired UAVs. ESC systems are appealing for characterizations in biological systems and applications to bio-mimicry due to their ability to describe naturally the steering of systems to optimal state as done by many animals, birds, and bugs. Moreover, ESC systems require only measurements of the objective function, which is, arguably, what many of said creatures do for dynamic optimization based on their sensing (measurements). *We believe this paper can encourage, and give insights, for more studies and lines of research on discovering and revealing extremum seeking systems in nature.*

Organization of the paper: In section 2, we provide the DS problem description and setup. In section 3, the extremum seeking system characterization of the DS problem is provided. This includes, the utilized ESC structures, stability of the ESC system, simulation results, and comparison with the numerical optimizers GPOPS2 [33] and DC [14] method. Section 4 concludes the paper and provide a future prospective.

2. Dynamic soaring problem description and setup

The DS problem is almost exclusively introduced as a nonlinear optimal control problem in literature [4]. Therefore, we will briefly provide the DS problem below as usually done in the literature and required for the numerical optimizers we use for comparisons in this paper. It is important to emphasize that *the ESC systems we introduce in section 3 will not require any of the constraints or bounds introduced here*.

2.1. Wind shear model

Wind shear takes place on thin layers between two regions in the atmosphere if the airflow vector is different. Wind shear is a prerequisite for energy extraction via DS [4, 14, 34]. So, it is important to have a proper model to describe the wind dynamics as per most dynamic optimization methods and numerical optimizers applied to DS [4]. In this work, we model the wind dynamics by a logistic function similar to [14]:

$$W(z) = \frac{W_0}{1 + e^{-z/\delta}}. \quad (1)$$

This wind model (graphically depicted in figure 2) is parameterized by free stream wind speed W_0 and shear layer thickness δ . It captures the main features of separated winds

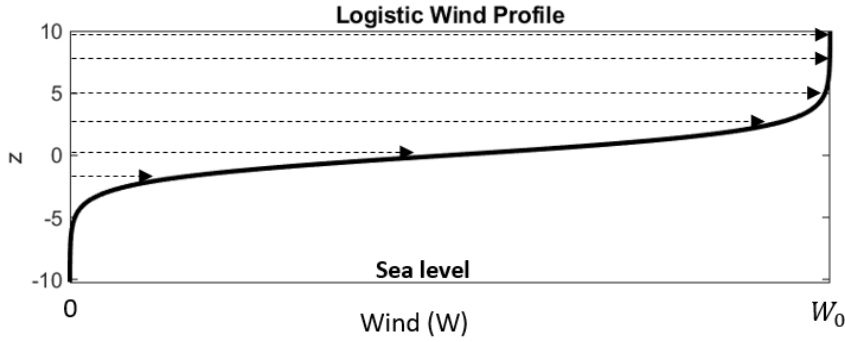


Figure 2. An example of a logistic wind profile with sea level at $z = -10$.

over ocean waves as well as features of any flow with a typical wind inhomogeneity W_0 developing over a length δ [14]. If the thickness of shear layer δ is very thin, this model approaches Rayleigh's discontinuous wind model.

2.2. Flight dynamics model

In this paper, we use a three-dimensional point-mass model with no thrust component, to represent an albatross or a mimicking UAV. It is important to note here that some researchers have used six degrees of freedom models [35]. We follow the assessment in the review work [4] that the improved accuracy using six degrees of freedom models would not substitute the increased computational complexity and expense when compared with

the three-dimensional point-mass model. The model used in this work is represented by the following system of differential equations [14]:

$$\begin{aligned}
\dot{x} &= V \cos \gamma \cos \psi, \\
\dot{y} &= V \cos \gamma \sin \psi - W, \\
\dot{z} &= V \sin \gamma, \\
m\dot{V} &= -D - mg \sin \gamma + m\dot{W} \cos \gamma \sin \psi, \\
mV\dot{\gamma} &= L \cos \phi - mg \cos \gamma - m\dot{W} \sin \gamma \sin \psi, \\
mV\dot{\psi} \cos \gamma &= L \sin \phi + m\dot{W} \cos \psi.
\end{aligned} \tag{2}$$

Our formulation, similar to [14], follows East, North and Up frame of reference, i.e. $(i, j, k) = (e_{East}, e_{North}, e_{Up})$ as shown in figure 3. Here, ψ is the angle between i and projection of V in ij -plane, and γ is the angle between V and ij -plane with nose up as positive. We assume the wind is blowing from North to South all the time and only a horizontal wind component exists. In our model, the speed and angles of albatross/UAV are modeled in wind relative reference and position (x, y, z) is modeled in Earth fixed-frame. We calculate the lift and drag forces using the following equations.

$$\begin{aligned}
L &= \frac{1}{2}\rho V^2 S C_D, \\
D &= \frac{1}{2}\rho V^2 S C_L,
\end{aligned} \tag{3}$$

where the parabolic drag coefficient is given by $C_D = C_{D0} + KC_L^2$. Table 2 provides the albatross flight dynamic characteristics.

Parameter	Value
m	9.5 kg
S	0.65 m^2
C_{D0}	0.01
K	0.0156
ρ	1.2 kg/m^3
g	9.8 m/s^2
W_0	7.8 m/s
δ	7 m

Table 2. Characteristics of the albatross used in this study.

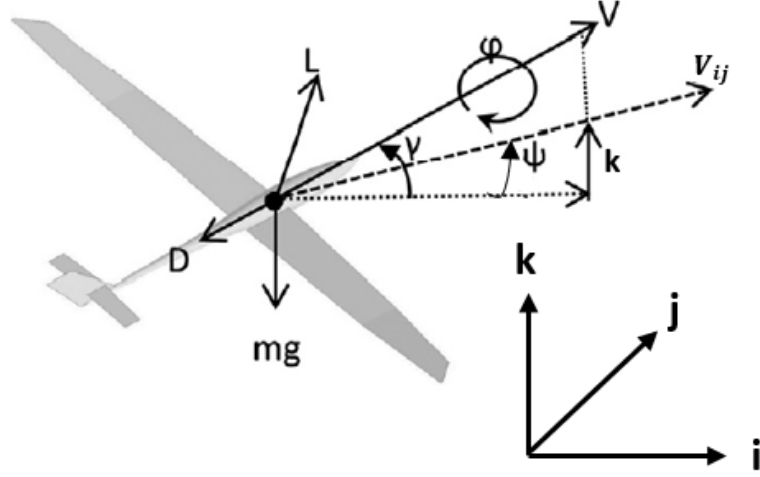


Figure 3. Aerodynamic forces acting on the UAV and the aerodynamic angles.

2.3. Problem formulation

We formulate the DS here as nonlinear optimal control problem as typically done in literature [4]. We define the state vector $\mathbf{x}(t)$ and the control vector $\mathbf{u}(t)$ as

$$\begin{aligned}\mathbf{x}(t) &= [x, y, z, V, \gamma, \psi], \\ \mathbf{u}(t) &= [C_L, \phi].\end{aligned}\tag{4}$$

The flight dynamic model in (2) with the wind profile in (1) can be configured as a nonlinear system of the form

$$\dot{\mathbf{x}}(t) = \mathbf{f}(\mathbf{x}(t), \mathbf{u}(t)).\tag{5}$$

Finally, the performance index to be maximized (or minimized) - the objective function - is denoted as $J = g(\mathbf{x}; \dot{W})$. It is a function of the state vector and wind shear gradient and is subject to boundary and path constraints. Some of the candidates of performance index are

$$\begin{aligned}J &= \min(W_0), \\ J &= \min(T_{cyc}), \\ J &= \max(Energy)_{gain}, \\ J &= \min(Thrust) \text{ or } \min(Power).\end{aligned}\tag{6}$$

Boundary conditions vary with different modes of dynamic soaring. For the basic dynamic soaring mode [4], the boundary constraints are

$$[z, V, \gamma, \psi]_{t_f}^T = [z + \Delta z, V, \gamma, \psi]_{t_0}^T,\tag{7}$$

where t_f and t_0 refer to final and initial times respectively and Δz is the net change in altitude after the cycle. Similarly, path constraints for states and control during the DS maneuver are presented in (8).

$$\begin{aligned} V_{\min} < V < V_{\max}, \psi_{\min} < \psi < \psi_{\max}, \\ \gamma_{\min} < \gamma < \gamma_{\max}, x_{\min} < x < x_{\max}, \\ y_{\min} < y < y_{\max}, z_{\min} < z < z_{\max}, \\ \phi_{\min} < \phi < \phi_{\max}, C_{L\min} < C_L < C_{L\max}. \end{aligned} \quad (8)$$

Since DS maneuver generates high accelerations, an additional path constraint of load factor is added as

$$n = \frac{L}{W} \leq n_{\max}. \quad (9)$$

3. Extremum seeking control systems characterize the dynamic soaring phenomenon

ESC is a model-free adaptive control technique that stabilizes a dynamical system around the extremum point of an objective/cost function [18, 22]. The design and main blocks of an ESC performing dynamic optimization is presented in its classical structure [19] in figure 4. The parameter θ is what the ESC is updating to reach the extremum of the objective function $J = g(\mathbf{x}; \theta)$. The ESC classic structure consists of three main steps. In the first step, a perturbation signal (modulation) is added to a nominal value of the parameter $\hat{\theta}$, which is an estimation for θ . The generated θ is fed into the system dynamics, which then provides a new evaluation (measurement) of the objective function J . In the second step, the evaluated value J is demodulated using a perturbation signal of the same frequency. The result of that determines if the estimation of θ needs to increase or decrease. In the third and final step, the demodulated value is integrated with the nominal value to update the parameter $\hat{\theta}$. In the next subsection, we hypothesize how the DS phenomenon can be characterized using ESC structures.

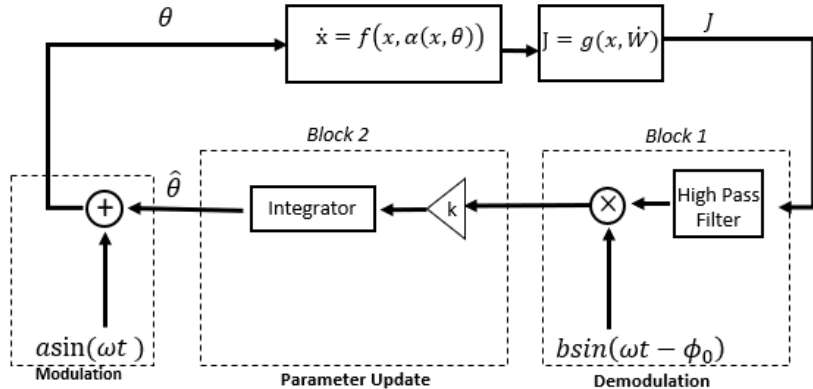


Figure 4. Classic structure design of an ESC.

3.1. Philosophy behind characterizing DS as an ESC

Soaring birds, as typically done by albatrosses [4], travel hundreds of miles using minimum to no effort in flying. This implies that they should have a mechanism and process that enables them to find a path that maximizes the energy gained from the wind so that they minimize the effort (energy spending) in flying. It is also important to note that they find that path autonomously and in real-time. A natural way to perform such a maneuver - assuming the presence of wind shear - is to first take a small variation/perturbation in pitching and/or rolling action/control, and then by sensing/measuring the corresponding changes in wind, velocity and height, the bird determines its energy state and whether it needs to change actions. Then, the actions are updated and the process is autonomously performed. The above-mentioned hypothesis matches that of extremum seeking systems. Figure 5 draws parallelism between the DS phenomenon and ESC systems. The pitching and rolling variation/perturbation action taken by the bird can be considered as the modulation step. Then, sensing the change in the wind, velocity and height is similar to measuring the objective function that extremum seeking systems do not require its mathematical expression as a priori. Finally, updating the action as per the feedback is similar to the demodulation and parameter update step. Consequently, ESC can be considered a natural control structure and mechanism to perform DS maneuvers. In the next subsections, we show that the DS phenomenon is an extremum seeking system in nature, and ESC designs are successful in achieving it.

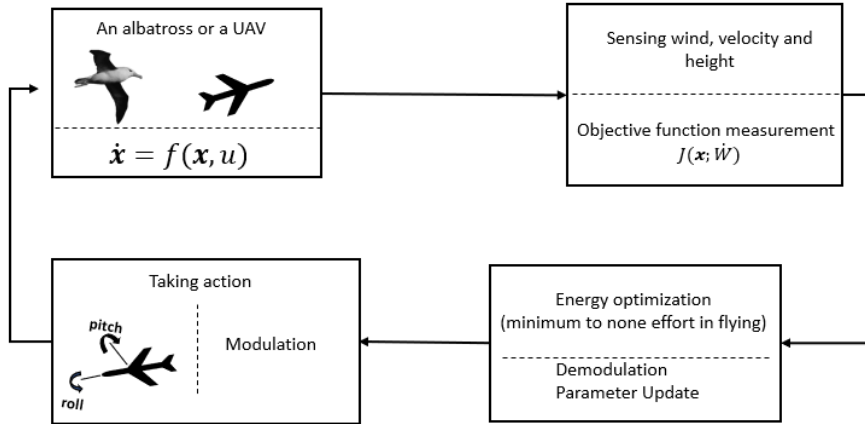


Figure 5. Parallelism between DS and ESC.

3.2. Structures of ESC characterizing and performing DS

The control inputs for the DS system are typically $\mathbf{u}(t) = [C_L, \phi]$ as shown in (4). However, the maneuver can be performed with free (varying) control of C_L as well as constant C_L as shown in [12]. We choose the case with constant C_L to make the DS

problem a Single Input Single Output (SISO) system with ϕ as the free (varying) control input. This allows us to take advantage of the mature and developed tools for SISO ESCs available in ESC literature. It is also our assessment that since ESC application to the DS problem is novel and without precedents, the introductory results of this problem are better to be on a SISO basis. The structure of ESC shown in figure 6 is used for this work. This structure is similar to [20, 21]. The use of this structure has been identified and selected for three technical reasons: (1) it allows for fast-tracking of the output, which is arguably what the bird is doing to avoid deflecting away from its optimized flight path, (2) it guarantees stability if certain assumptions and conditions (verifiable and can be constructed by design) are satisfied, unlike many other ESC structures where the stability property is characterized by existence theorems and conditions that are hard to verify or construct a proof for them, and (3) *it allows the optimal input and optimal output (objective function) to be time-varying, which matches the nature of the DS problem that maximizes or minimizes its output as a function of time*. It is worth noting that the selected ESC structure, which is not found in many applications, is different from most other ESCs that are operable for static maps (time-invariant objective functions) [22]. We here set the parameter maximizing or minimizing the objective function $J = g(\mathbf{x}, \dot{W})$ as $\theta = \phi$, so that $\alpha(\mathbf{x}, \theta) = \phi$. We denote the optimal input and output as ϕ^* and J^* respectively. Now, their Laplace transforms are denoted as

$$\begin{aligned} L[\phi^*(t)] &= \lambda_\phi \Gamma_\phi(s) \\ L[J^*(t)] &= \lambda_J \Gamma_J(s), \end{aligned} \tag{10}$$

where λ_ϕ and λ_J are constants. If ϕ^* and θ^* are constants (step functions), then the structure in figure 6 is equivalent, and reduces, to the classic structure [19] in figure 4. Following the design steps of Algorithm 2.1 in [21], we need to make an assumption on the nature of $\theta^*(t)$ and the nature of $J^*(t)$. These assumptions are not the “equivalent” expression for $\theta^*(t)$ and $J^*(t)$. As a matter of fact, neither $\theta^*(t)$ nor even $J^*(t)$ need to be known a priori. From many observations made on DS maneuvers, theoretically as in [13, 1, 2, 14] and experimentally as in [3, 6], one can deduce that the nature of $\theta^*(t)$ and $J^*(t)$ will be periodic and sinusoidal-like. Moreover, in the controllability study published recently on DS [34], it was shown that the DS problem can be formulated as a control-affine system of the form (11):

$$\dot{\mathbf{x}} = \mathbf{b}_0(\mathbf{x}) + \sum_{i=1}^m u_i \mathbf{b}_i(\mathbf{x}), \tag{11}$$

where $\mathbf{x} \in \mathbb{R}^n$ is the state space vector, \mathbf{b}_0 is the drift (uncontrolled) vector field of the system, u_i are the control inputs and $\mathbf{b}_i(\mathbf{x})$ are the control vector fields for m number of controls. Given that we are dealing with an SISO system, the only control input variation we can apply will be through $\theta = \phi$. The controllability of the system (11) requires control inputs that satisfy the condition: if $U \in \mathbb{R}^m$ is the set of admissible controls then for every u_i we have $u_i : I \rightarrow U$ for $I \subset \mathbb{R}$ and they

are locally integrable and also $\mathbf{0} \in \text{int}(\text{conv}(U))$ (see chapter 7, [36]). This condition needs to be satisfied in order for the so called “Lie bracket proper variations” to take place. Now, as shown in [37, 38], sinusoidal inputs are typical candidates to cause the control inputs variations which cause steering/motion-planning of the system and provide controllability. Driven by the above-mentioned observations and reasoning, we assume the optimal input and output nature as sinusoidal signals with phase shift, i.e. $\theta^*(t) = \sin(a_0 t + b_0)$ and $J^*(t) = \sin(c_0 t + d_0)$, where a_0, b_0, c_0, d_0 are some parameters. By using Laplace transform we find

$$\begin{aligned}\Gamma_J &= \frac{a_0 \cos b_0 + s \sin b_0}{a_0^2 + s^2} \\ \Gamma_\phi &= \frac{c_0 \cos d_0 + s \sin d_0}{c_0^2 + s^2}.\end{aligned}\tag{12}$$

Next, the compensators C_0 and C_i in block 1 and block 2 in figure 6 are designed following the algorithm 2.1 presented in [21]. We assume $F_0(s)$ and $F_i(s)$ in figure 1 in [21] as “1”. We further discuss the stability analysis of this structure in sub-section 3.4. Since DS can be seen as a slow system that represents the flight dynamics of a fairly large bird (albatross) and it takes a relatively long time to perform its cycle, we are also going to implement the problem using the classic structure in figure 4 which can work for some time-varying outputs, especially when the system dynamics is slow.

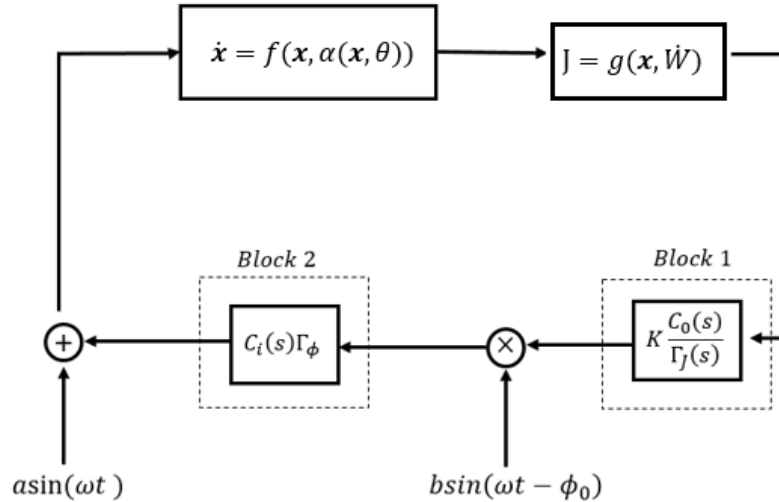


Figure 6. ESC structure used for dynamic soaring.

3.3. Simulations and comparative results

We perform simulations for two different structures of ESCs and compare the result with the solutions obtained from two numerical optimizers. The two ESC structures are the ESC structure in figure 6 (referred as “ESC1”) and the ESC structure in figure 4 (referred

as “ESC2”). The first numerical optimizer we used is GPOPS2 [33], an optimization software compatible with MATLAB®, while the second numerical optimizer we used is Direct Collocation (DC) method-based optimizer in Python. For the DC optimizer, we followed a process in implementation similar to the supplementary material of [14]. Among the candidates of performance index - objective functions - presented in (6), we choose the expression corresponding to specific energy gain, $J = -V\dot{W} \cos \gamma \sin \psi / g$ to be maximized. The expression of the performance index is derived here. We define specific energy as total energy per weight, such that

$$e = E/mg = z + \frac{V^2}{2g}. \quad (13)$$

Now, taking derivative with respect to time, we get

$$\dot{e} = \dot{z} + \frac{V\dot{V}}{g} \quad (14)$$

$$= V \sin \gamma + \frac{V}{g} [-D - g \sin \gamma - \dot{W} \cos \gamma \sin \psi] \quad (15)$$

$$= -\frac{DV}{g} - \frac{V\dot{W} \cos \gamma \sin \psi}{g}. \quad (16)$$

According to (16), the term $-V\dot{W} \cos \gamma \sin \psi / g$ is the one determining energy gain from the wind. We use this performance index measure for both ESC structures and GPOPS2, whereas for the DC method of optimization, we do not use the performance index measure and solve it as the “constraints satisfaction” problem as done in [14]. For some optimal control problems in DS literature, the problem is so heavily constrained that it does not require an objective function. This is a problem, we hope this work will help to resolve. *It is important to emphasize that all bounds and constraints in (7), (8) and (9) are not applied or required in ESC1 and ESC2, however, they are a must for GPOPS2 and DC method.*

For ESC1, we design the block 1 as $(s^2 + 1.5^2)/((s + 0.4)(s + 2))$ and block 2 as $0.01(s \sin 2.5 + \cos 2.5)/(s^2 + 1)$. Now, for the modulating signal, we use a frequency of $\omega = 1$ and amplitude of $a = 1$, and the demodulating signal has the same frequency with the amplitude of $b = 2$ and phase shift ($\phi_0 = 0$). We apply a constant $C_L = 1.4$. Similarly, for ESC2, we assume block 1 as $s/(s+3)$ and block 2 as $0.6/s$. The modulating signal has a frequency of $\omega = 1$ and amplitude of $a = 0.8$, whereas the demodulating signal has the same frequency with an amplitude of $b = 1.6$ and phase shift $\phi_0 = -125^\circ$. We apply, similar to ESC1, $C_L = 1.4$. The parameters of the albatross flight dynamics and wind model are provided in table 2. The initial state of the simulation is taken as $[x, y, z, V, \gamma, \psi] = [-16, 15, 0, 14, -0.4, -1.16]$ and it is fixed for all simulations. We run the simulation for one cycle of DS. It is important to mention here that ESC – as it is the case in most controllers – requires tuning of parameters, which is a challenge. So, for the choice of parameters in the simulations, we have followed the guidelines presented in algorithm 2.1 in [21] and tuned them for optimal results. The results of our simulation implementing ESC1, ESC2, GPOPS2 and DC are presented in figures 7, 8 and 9.

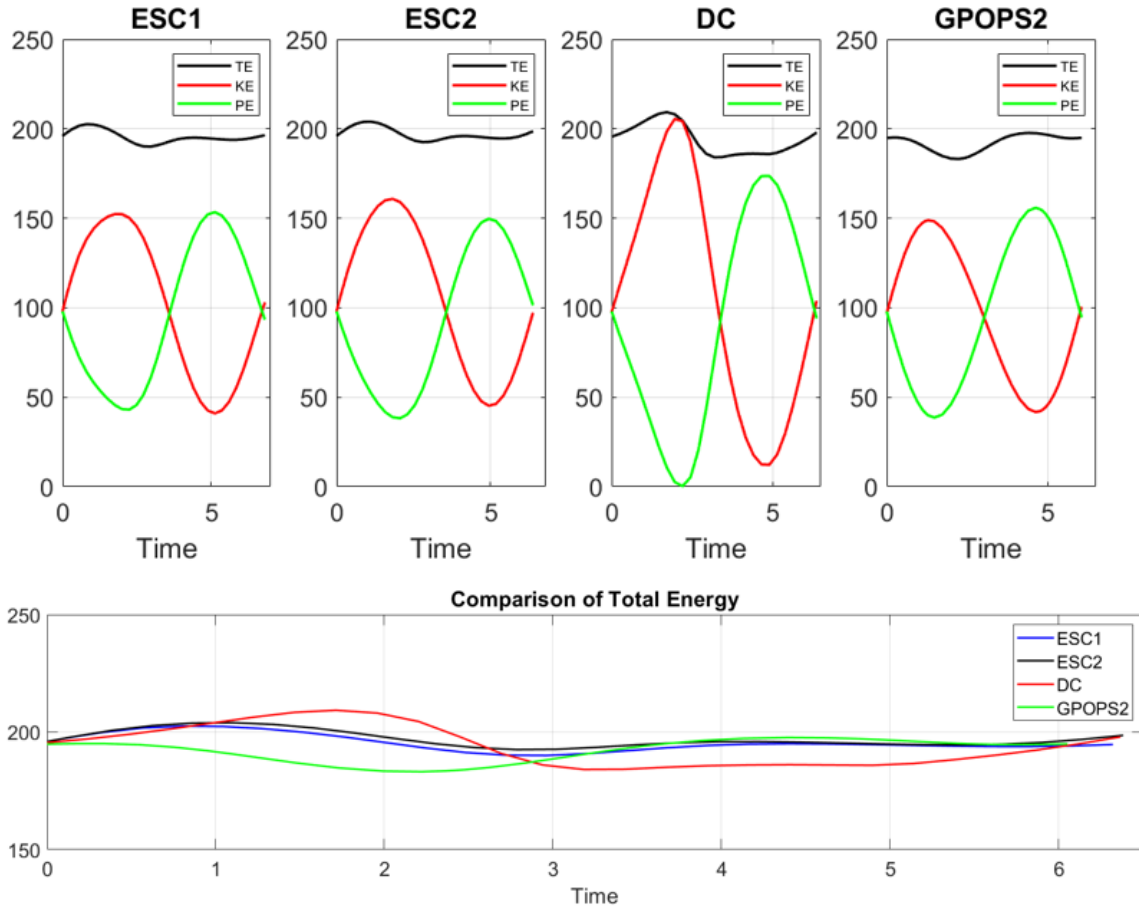


Figure 7. Comparison of total energy during a cycle of dynamic soaring obtained using ESC1, ESC2, GPOPS2 and DC methods.

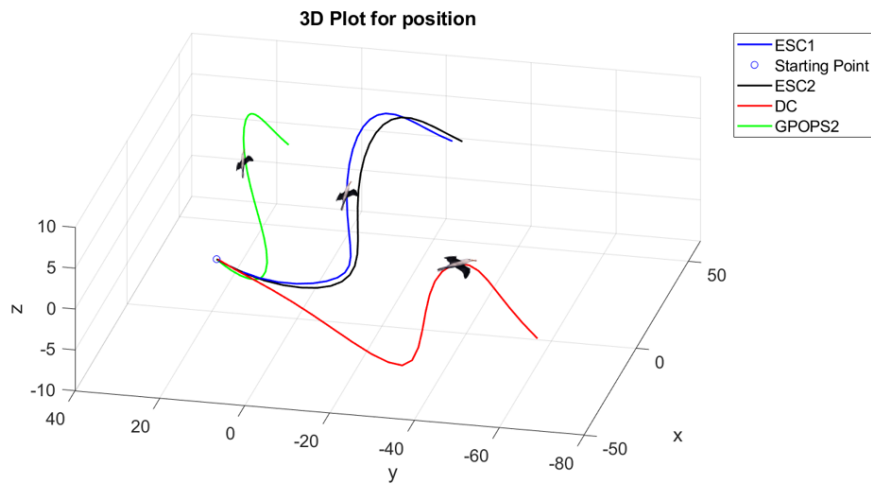


Figure 8. Comparison of trajectories of albatross obtained using ESC1, ESC2, GPOPS2 and DC methods.

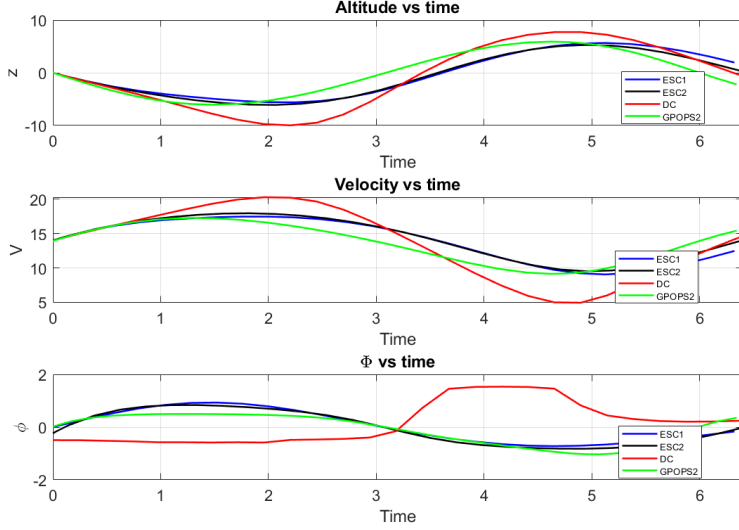


Figure 9. Comparison of velocity, altitude and control input ϕ of albatross obtained using ESC1, ESC2, GPOPS2 and DC methods.

Figure 7 represents the most important indication of the success of our implementation. That is, *the absolute and most important characteristic of the DS phenomenon is the energy neutrality*. In other words, the DS is achieved if the KE is traded off with the PE and vice versa without any loss to drag, i.e., the system is conservative, unlike typical flight dynamic systems which are dissipative systems due to drag. Figure 7 provides a comparison between PE, KE and TE obtained during the dynamic soaring cycle using all of the four methods considered in the implementation. It can be observed that the total energy is near-constant in all of the four methods. Figures 8 and 9 show the comparison between 3D trajectories, velocity, altitude and the control input ϕ obtained using all four methods. Results obtained via all methods are comparable except for the trajectory obtained using the DC method, as it is progressing in a different direction. This might be because, using the DC optimizer as in [14], is without maximizing any performance index measure (no objective function, only constraints). Even though the results are similar in achieving energy neutrality, the application of ESC represents strong and novel benefits to the DS problem. For example, the controller is autonomous and acts in a real-time, with no need for the constraints and bounds in (7),(8) and (9), unlike the numerical optimizers GPOPS2 and DC. Additionally, the controller is much simpler and appears to be very natural to this nature-inspired phenomenon. As a summary of the difference in control characteristics, a comparison between ESC structures and numerical optimizers such as GPOPS2 is presented in table 3.

3.4. Determining the stability of the ESC1 structure

We define the following assumptions and conditions C1-C5 as in [21]:

Performance criterion	ESC Structures	Numerical Optimizers such as GPOPS2
Functionality in Real time.	Work in real time.	Do not work in real time.
Nature of the objective function.	Measured value of the objective function is enough and does not necessitate the mathematical expression a priori.	Needs mathematical expression of the objective function being maximized (or minimized).
Design parameters and constraints.	Few design parameters and no constraints.	Heavy amount of parameters, bounds and constraints are needed to define the problem.
Stability.	Stable.	Not necessarily Stable [16, 17].

Table 3. Comparison of proposed ESC structures with other numerical optimizers on various criteria.

- C1. $F_i(s)$ and $F_0(s)$ are asymptotically stable and proper.
- C2. $\Gamma_J(s)$ and $\Gamma_\phi(s)$ are strictly proper rational functions and the poles of $\Gamma_\phi(s)$ that are not asymptotically stable are not zeros of $C_i(s)$.
- C3. Zeros of $\Gamma_J(s)$ that are not asymptotically stable are also zeros of $C_0(s)$.
- C4. $C_0(s)/\Gamma_J(s)$ and $C_i(s)\Gamma_\phi(s)$ are proper.
- C5. $C_0(s)$ and $1/(1 + L(s))$ are asymptotically stable, where $L(s) = af''/4 \cdot H_i(s)[Re(e^{j\phi_0} F_i(j\omega) H_0(s + j\omega))]$ and $H_i = C_i(s)\Gamma_\phi(s)F_i(s)$, $H_0(s) = C_0(s)/\Gamma_J(s) \cdot F_0(s)$, f'' is constant.

Theorem 1: The output error $\tilde{J} = J - J^*$ in the ESC1 structure in figure 6 achieves local exponential convergence to an $O(a^2 + 1/\omega^2)$ neighborhood of origin.

Proof: Since $F_i(s) = 1$ and $F_0(s) = 1$ are asymptotically stable and proper, the condition C1 is satisfied. Similarly, Γ_J and Γ_ϕ as defined in (12) are strictly proper rational functions. So, the condition C2 is also satisfied. In addition, we designed $C_i = 0.01$, $C_i(s)\Gamma_\phi = 0.01(s \sin 2.5 + \cos 2.5)/(s^2 + 1)$, and $C_0(s)/\Gamma_J = (s^2 + 1.5^2)/((s + 0.4)(s + 2))$, as defined in section 3.3. As a result, conditions C2-C5 are all satisfied. Now, as per Theorem 2.1 in [21], satisfaction of conditions C1-C5 completes the proof.

Remark: The structure in figure 6 is a member of the family of reduced structures from the generalized structure in [21]. Thus, the proof presented in Appendix B of [21] applies to the ESC1 structure as well.

4. Conclusive remarks and future works

This paper provides a novel framework and original insights for future research in two fundamental ways. The first fundamental is regarding the DS problem itself and the enabling of bio-mimicry of albatross, and other soaring birds, by UAVs. *The results of this paper, remarkably, provide an unconstrained, real-time, autonomous, stable, and simple control solution for the DS problem that is also not requiring the mathematical expression of the objective function a priori.* The second fundamental is regarding the topic of extremum seeking in nature. The process and mechanisms many birds, animals, and bugs are conducting to reach optimally (through dynamic optimization) their objective is, arguably, can be seen as an extremum seeking system mechanism. *Creatures in nature cannot be conducting non-real-time, unstable, or very complex procedures due to the lack of resources and ability. We believe this paper contributes to the legitimacy of the above-mentioned hypothesis that many of nature creatures are conducting extremum seeking processes.* In the future, we are aiming at implementing the DS problem in more real situations where we do not have ideal wind shear or the absence of its model to further test the ESC application to a mimicking UAV. Also, more research needs to be done on sensing and how one would take measurements of wind shear to enable ESC implementation. We believe this paper will encourage us and others to pursue more investigations of natural phenomena that can be characterized by extremum seeking systems.

References

- [1] C. Gao and H. H. Liu, “Dubins path-based dynamic soaring trajectory planning and tracking control in a gradient wind field,” *Optimal Control Applications and Methods*, vol. 38, no. 2, pp. 147–166, 2017.
- [2] I. Mir, A. Maqsood, H. E. Taha, and S. A. Eisa, “Soaring energetics for a nature inspired unmanned aerial vehicle,” in *AIAA Scitech 2019 Forum*, 2019, p. 1622.
- [3] G. Sachs, J. Traugott, A. Nesterova, and F. Bonadonna, “Experimental verification of dynamic soaring in albatrosses,” *Journal of Experimental Biology*, vol. 216, no. 22, pp. 4222–4232, 2013.
- [4] I. Mir, S. A. Eisa, and A. Maqsood, “Review of dynamic soaring: technical aspects, nonlinear modeling perspectives and future directions,” *Nonlinear Dynamics*, pp. 1–28, 2018.
- [5] P. L. Richardson, “How do albatrosses fly around the world without flapping their wings?” *Progress in Oceanography*, vol. 88, no. 1-4, pp. 46–58, 2011.
- [6] Y. Yonehara, Y. Goto, K. Yoda, Y. Watanuki, L. C. Young, H. Weimerskirch, C.-A. Bost, and K. Sato, “Flight paths of seabirds soaring over the ocean surface enable measurement of fine-scale wind speed and direction,” *Proceedings of the National Academy of Sciences*, vol. 113, no. 32, pp. 9039–9044, 2016.
- [7] P. L. Richardson, “Leonardo da vinci’s discovery of the dynamic soaring by birds in wind shear,” *Notes and Records: the Royal Society journal of the history of science*, vol. 73, no. 3, pp. 285–301, 2019.
- [8] Y. J. Zhao, “Optimal patterns of glider dynamic soaring,” *Optimal control applications and methods*, vol. 25, no. 2, pp. 67–89, 2004.
- [9] M. Deittert, A. Richards, C. A. Toomer, and A. Pipe, “Engineless unmanned aerial vehicle propulsion by dynamic soaring,” *Journal of guidance, control, and dynamics*, vol. 32, no. 5, pp. 1446–1457, 2009.

- [10] P. P. Sukumar and M. S. Selig, "Dynamic soaring of sailplanes over open fields," *Journal of Aircraft*, vol. 50, no. 5, pp. 1420–1430, 2013.
- [11] J. J. Bird, J. W. Langelaan, C. Montella, J. Spletzer, and J. L. Grenestedt, "Closing the loop in dynamic soaring," in *AIAA Guidance, Navigation, and Control Conference*, 2014, p. 0263.
- [12] G. Sachs, "Minimum shear wind strength required for dynamic soaring of albatrosses," *Ibis*, vol. 147, no. 1, pp. 1–10, 2005.
- [13] I. Mir, A. Maqsood, S. A. Eisa, H. Taha, and S. Akhtar, "Optimal morphing-augmented dynamic soaring maneuvers for unmanned air vehicle capable of span and sweep morphologies," *Aerospace Science and Technology*, 2018.
- [14] G. D. Bousquet, M. S. Triantafyllou, and J.-J. E. Slotine, "Optimal dynamic soaring consists of successive shallow arcs," *Journal of The Royal Society Interface*, vol. 14, no. 135, p. 20170496, 2017.
- [15] D.-X. Wang, F.-F. Xie, Y.-F. Lu, T.-W. Ji, C.-P. Du, and Y. Zheng, "Bio-inspired dynamic soaring simulation system with distributed pressure sensors," *Bioinspiration & Biomimetics*, 2022.
- [16] I. Mir, S. A. Eisa, H. Taha, A. Maqsood, S. Akhtar, and T. U. Islam, "A stability perspective of bioinspired unmanned aerial vehicles performing optimal dynamic soaring," *Bioinspiration & Biomimetics*, vol. 16, no. 6, p. 066010, 2021.
- [17] I. Mir, F. Gul, S. Eisa, A. Maqsood, and S. Mir, "Contraction analysis of dynamic soaring," in *AIAA SCITECH 2022 Forum*, 2022, p. 0881.
- [18] Y. Tan, W. Moase, C. Manzie, D. Nešić, and I. Mareels, "Extremum seeking from 1922 to 2010," in *Proceedings of the 29th Chinese Control Conference*, 2010, pp. 14–26.
- [19] M. Krstić and H.-H. Wang, "Stability of extremum seeking feedback for general nonlinear dynamic systems," *Automatica*, vol. 36, no. 4, pp. 595–601, 2000. [Online]. Available: <https://www.sciencedirect.com/science/article/pii/S0005109899001831>
- [20] M. Krstić, "Performance improvement and limitations in extremum seeking control," *Systems & Control Letters*, vol. 39, no. 5, pp. 313–326, 2000.
- [21] K. B. Ariyur and M. Krstic, "Analysis and design of multivariable extremum seeking," in *Proceedings of the 2002 American Control Conference (IEEE Cat. No. CH37301)*, vol. 4. IEEE, 2002, pp. 2903–2908.
- [22] ———, *Real-time optimization by extremum-seeking control*. John Wiley & Sons, 2003.
- [23] D. F. Chichka, J. L. Speyer, C. Fanti, and C. G. Park, "Peak-seeking control for drag reduction in formation flight," *Journal of Guidance, Control, and Dynamics*, vol. 29, no. 5, pp. 1221–1230, 2006. [Online]. Available: <https://doi.org/10.2514/1.15424>
- [24] E. Biyik and M. Arcak, "Gradient climbing in formation via extremum seeking and passivity-based coordination rules," in *2007 46th IEEE Conference on Decision and Control*, 2007, pp. 3133–3138.
- [25] J. Cochran and M. Krstic, "Nonholonomic source seeking with tuning of angular velocity," *IEEE Transactions on Automatic Control*, vol. 54, no. 4, pp. 717–731, 2009.
- [26] S. L. Brunton, C. W. Rowley, S. R. Kulkarni, and C. Clarkson, "Maximum power point tracking for photovoltaic optimization using extremum seeking," in *2009 34th IEEE Photovoltaic Specialists Conference (PVSC)*, 2009, pp. 000 013–000 016.
- [27] R. Leyva, C. Alonso, I. Queinnec, A. Cid-Pastor, D. Lagrange, and L. Martinez-Salamero, "Mppt of photovoltaic systems using extremum - seeking control," *IEEE Transactions on Aerospace and Electronic Systems*, vol. 42, no. 1, pp. 249–258, 2006.
- [28] S. Drakunov, U. Ozguner, P. Dix, and B. Ashrafi, "Abs control using optimum search via sliding modes," *IEEE Transactions on Control Systems Technology*, vol. 3, no. 1, pp. 79–85, 1995.
- [29] E. Dinçmen, B. A. Güvenç, and T. Acarman, "Extremum-seeking control of abs braking in road vehicles with lateral force improvement," *IEEE Transactions on Control Systems Technology*, vol. 22, no. 1, pp. 230–237, 2014.
- [30] B. Zhou, J. Ke, Z. Han, and X. Guan, "A review of extremum seeking control or source seeking control and its application of mobile robot," in *2019 IEEE 9th Annual International Conference*

on CYBER Technology in Automation, Control, and Intelligent Systems (CYBER). IEEE, 2019, pp. 1541–1546.

- [31] J. Cochran, E. Kanso, S. D. Kelly, H. Xiong, and M. Krstic, “Source seeking for two nonholonomic models of fish locomotion,” *IEEE Transactions on Robotics*, vol. 25, no. 5, pp. 1166–1176, 2009.
- [32] H. Nakadai, D. Sobey, M. Yamakita, and T. Mukai, “Liquid environment-adaptive ipmc fish-like robot using extremum seeking feedback,” in *2008 IEEE/RSJ International Conference on Intelligent Robots and Systems*. IEEE, 2008, pp. 3089–3094.
- [33] M. A. Patterson and A. V. Rao, “Gpops-ii: A matlab software for solving multiple-phase optimal control problems using hp-adaptive gaussian quadrature collocation methods and sparse nonlinear programming,” vol. 41, no. 1, oct 2014.
- [34] I. Mir, H. Taha, S. A. Eisa, and A. Maqsood, “A controllability perspective of dynamic soaring,” *Nonlinear Dynamics*, vol. 93, pp. 1–16, 2018.
- [35] N. Akhtar, A. K. Cooke, and J. F. Whidborne, “Positioning algorithm for autonomous thermal soaring,” *Journal of aircraft*, vol. 49, no. 2, pp. 472–482, 2012.
- [36] F. Bullo and A. D. Lewis, *Geometric control of mechanical systems: modeling, analysis, and design for simple mechanical control systems*. Springer Science & Business Media, 2004, vol. 49.
- [37] H. J. Sussmann and W. Liu, “Lie bracket extensions and averaging: the single-bracket case,” in *Nonholonomic motion planning*. Springer, 1993, pp. 109–147.
- [38] H.-B. Dürr, M. S. Stanković, C. Ebenbauer, and K. H. Johansson, “Lie bracket approximation of extremum seeking systems,” *Automatica*, vol. 49, no. 6, pp. 1538–1552, 2013. [Online]. Available: <https://www.sciencedirect.com/science/article/pii/S0005109813000800>